

A multiscale model for tropical intraseasonal oscillations

Andrew J. Majda* and Joseph A. Biello

Courant Institute of Mathematical Sciences, Center for Atmosphere and Ocean Sciences, New York University, 251 Mercer Street, New York, NY 10012

Contributed by Andrew J. Majda, February 12, 2004

The tropical intraseasonal 40- to 50-day oscillation (TIO) is the dominant component of variability in the tropical atmosphere with remarkable planetary-scale circulation generated as envelopes of complex multiscale processes. A new multiscale model is developed here that clearly demonstrates the fashion in which planetary-scale circulations sharing many features in common with the observational record for the TIO are generated on intraseasonal time scales through the upscale transfer of kinetic and thermal energy generated by wave trains of organized synoptic-scale circulations having features in common with observed superclusters. The appeal of the multiscale models developed below is their firm mathematical underpinnings, simplicity, and analytic tractability while remaining self-consistent with key features of the observational record. The results below demonstrate, in a transparent fashion, the central role of organized vertically tilted synoptic-scale circulations in generating a planetary circulation resembling the TIO.

The dominant component of intraseasonal variability in the tropics is the 40- to 50-day tropical intraseasonal oscillation (TIO), often called the Madden-Julian oscillation (MJO) after its discoverers (1). In the troposphere, the MJO is an equatorial planetary-scale wave envelope of complex multiscale convective processes that begins as a standing wave in the Indian Ocean and propagates across the Western Pacific at a speed of $\approx 5 \text{ ms}^{-1}$ (2–5). The planetary-scale circulation anomalies associated with the MJO significantly affect monsoon development and intraseasonal predictability in mid-latitudes and impact the development of the El Niño southern oscillation (ENSO) in the Pacific Ocean, which is one of the most important components of seasonal prediction (6–8). Present-day computer general circulation models (GCMs) typically poorly represent the MJO (9). One conjecture for the reason for this poor performance of GCMs is the inadequate treatment across multiple spatial scales of the interaction of the hierarchy of organized structures that generate the MJO as their envelope.

There have been a large number of theories attempting to explain the MJO through a specific linearized mechanism such as evaporation wind feedback (10, 11), boundary layer frictional convective instability (12), stochastic linearized convection (13), radiation instability (14), and the planetary-scale linear response to moving heat sources (15). Moncrieff (16) recently developed an interesting phenomenological nonlinear theory for the upscale transport of momentum from equatorial mesoscales [$O(300 \text{ km})$] to planetary scales and applied this theory to explain the “MJO-like” structure in recent “super-parametrization” computer simulations (17) with a scale gap (no resolution at all) on scales between 200 and 1,200 km. Despite all of these interesting contributions, the problem of explaining the MJO has recently been called the search for the Holy Grail of tropical atmospheric dynamics (14). Here we contribute to this search.

In this article, the viewpoint is adopted that since the MJO is a multiscale low frequency mode of tropical atmospheric motion, a fundamental challenge is to understand the role of interaction across scales in explaining the planetary response in the MJO. In mid-latitudes, the theory of baroclinic instability successfully describes the influence of coherent synoptic scales disturbances

on the planetary scales. In the tropics, superclusters (2, 18–20) are the documented coherent structures on the equatorial synoptic scales [$O(1,500 \text{ km})$], and the observations also indicate that the MJO is a propagating planetary-scale envelope of such superclusters (2). Here we develop a multiscale model that focuses on the planetary-scale circulation anomalies induced by the interaction with equatorial synoptic-scale circulations created by a wave train of superclusters. This is an analogue for the tropics of the mid-latitude baroclinic instability problem where the superclusters are the equatorial synoptic-scale disturbances and the MJO is predicted as the planetary-scale response through upscale transfer of kinetic and potential energy. The theoretical framework utilized below is the intraseasonal planetary equatorial synoptic dynamics (IPESD) model derived recently by A.J.M. and R. Klein (21). The IPESD model is a multiscale balanced model, systematically derived from the primitive equations through asymptotic mathematical procedures and provides simplified equations for the upscale transfer of energy from a wave train of equatorial synoptic-scale circulations to the planetary scale. Although the IPESD model is nonlinear, as shown below, it has solutions that are readily processed through exact solution formulas and elementary numerics. This simplicity is a major virtue of the present models as “thought process” models of the MJO for future investigations.

The outline of the remainder of the article is as follows. First, several detailed features of the MJO from observations are summarized, then the IPESD models for multiscale interaction are introduced briefly. Next, models for coherent equatorial synoptic-scale circulations in the western warm pool are developed, including one with organized coherent structures with key features of superclusters from observations and one without such structures. The planetary-scale response to such structures is studied subsequently through the IPESD multiscale model. In particular it is shown that only equatorial synoptic-scale circulations with the key features of supercluster wave trains induce a planetary-scale response in the model. For the organized supercluster wave trains on synoptic scales it is shown that many planetary-scale features of the MJO circulation from the observational record are generated through the multiscale models. Both standing wave solutions for the MJO formation phase and traveling wave solutions for the propagating phase are presented below. The article ends with a brief summary discussion.

Observed Features of the MJO

Some of the main characteristics of the observational record are the following:

- A. The planetary-scale filtered MJO envelope has a distinctive quadrupole flow structure. In the lower troposphere, there is

This paper was submitted directly (Track II) to the PNAS office.

Abbreviations: GCM, general circulation model; IPESD, intraseasonal planetary equatorial synoptic dynamics; MJO, Madden-Julian oscillation; QLELWE, quasilinear equatorial long-wave equations; SEWTG, synoptic-scale equatorial weak temperature gradient; TIO, tropical intraseasonal 40- to 50-day oscillation.

*To whom correspondence should be addressed. E-mail: jonjon@cims.nyu.edu.

© 2004 by The National Academy of Sciences of the USA

a symmetric leading pair of off-equatorial anticyclones extending to roughly $\pm 2,500$ km north and south of the equator with leading low-level easterly flow while the trailing flow is a cyclone pair extending to $\pm 2,500$ km north and south with a strong “westerly wind burst” region of flow on the equator. The upper-troposphere flow is a stronger antisymmetric version of the lower-level flow with cyclones and westerlies leading anticyclones and easterlies. Compare figure 2 and 3 of ref. 3, figure 3 of ref. 4, and phases 4 and 5 in figures 7 and 9 of ref. 5 with the multiscale model results in Figs. 4 and 5 below, which reproduce all of these flow features qualitatively.

- B. The MJO envelope structure in A is created as a standing wave in the Indian Ocean (see ref. 5, phases 3 and 4); the MJO slowly propagates across the Indian Ocean and Western Pacific at a rough speed of 5 ms^{-1} (2–5).
- C. The large-scale MJO is an envelope of equatorial synoptic-scale superclusters (2).
- D. The equatorial synoptic-scale dynamics in the MJO are driven by latent heating (22) with strengths of $5\text{--}10^\circ\text{K/day}$.
- E. In the lower troposphere the westerly wind burst region is strongest at heights around 4 or 5 km and weaker near the bottom of the troposphere above the boundary layer at heights around 0.5 km; thus, there is strong low-level vertical shear on the equator in the westerly windburst region (see figure 3 of ref. 23).

Since superclusters are the equatorial synoptic scale coherent structures associated with the planetary-scale MJO, it is useful for the theory developed below to briefly summarize their structure from the observational record (2, 18–20):

- F. Superclusters of organized convection have structure in the lower troposphere that varies between 1,500 and 3,000 km, i.e., on the equatorial synoptic scale (19, 20).
- G. The superclusters are equatorially trapped and move eastward at a phase speed of $\approx 15 \text{ ms}^{-1}$ (2, 18–20).
- H. The velocity and pressure structure in a supercluster has a pronounced upward vertical and westward tilt (18–20).

Relatively simple linear and nonlinear models with two vertical modes of heating are capable of reproducing key features of the superclusters (24, 25).

Finally, an interesting spectral analysis of the observational record (figure 3 of ref. 18 and figures 2, 3 c and d, and 9 of ref. 19) yields three prominent spectral peaks with behavior summarized below:

- I. There are two prominent low-frequency spectral peaks in the 40-day regime at planetary spatial scales. One is associated with the MJO and seems to have the dispersion relation $d\omega/dk = 0$; the second nearly symmetric peak is associated with large-scale equatorial Rossby waves (26).
- J. There is also a prominent spectral peak in the higher-frequency 10- to 20-day region associated with the superclusters discussed in F–H.

The IPESD Model

The fundamental model for the dynamical behavior of the troposphere assumed here is the constant buoyancy frequency Boussinesq equations with standard troposphere value for the buoyancy frequency, $N = 10^{-2} \text{ s}^{-1}$, and a tropospheric height of ≈ 16.5 km (26). Rigid lid boundary conditions with no vertical flow are assumed at the bottom of the free troposphere at height 0.5 km above the surface and at the top of the troposphere at 16.5 km. This is a simplified version of the primitive equations for the lower troposphere where both coupling to the boundary layer and also to the stratosphere are ignored. Under these circumstances, the natural reference speed, c_{ref} , is the gravity wave

speed of the first baroclinic vertical mode, $c = 50 \text{ ms}^{-1}$, and the standard equatorial synoptic length and time scales, l_s and T_s , are defined by $l_s = (c/\beta)^{1/2} = 1,500$ km and $T_s = (c\beta)^{-1/2} = 8.5$ h, where β represents the leading order curvature effect of the Earth at the equator (26). Below, (U, V, W) denote the x, y, z components of velocity also called the zonal, meridional, and vertical velocities, respectively, whereas the (x, y, z) coordinates are identified with the east–west or zonal, north–south or meridional, and vertical directions, respectively. The remaining dynamic variables are the pressure, P , and equivalent temperature, θ . Since the reference flow speed, $c = 50 \text{ ms}^{-1}$, is very large it is natural to consider flows for the equatorial primitive equations where the Froude number, defined by the ratio of typical horizontal velocity magnitudes and the basic wave speed, $Fr = v_{\text{ref}}/c = \varepsilon$, is a small parameter since values of ε in the range $0.1 \leq \varepsilon \leq 0.4$ give very reasonable flow velocities for the tropical troposphere. Intuitively, one regime of balanced dynamics occurs on the equatorial synoptic length scale, l_s , but on the larger advective time scale $T_1 = l_s/v_{\text{ref}}$, which is ≈ 3.5 days; since 10 units of this time scale span more than 1 month, T_1 is an intraseasonal time scale. Since the equatorial circumference is 40,000 km and the equatorial synoptic scale, l_s , is $\approx 1,500$ km, it is very natural to have envelope modulations of equatorial synoptic-scale behavior on the planetary scale, $X = \varepsilon x$. The simplified multiscale equations derived from the primitive equations under the above assumptions through systematic asymptotic principles are the IPESD equations (see pp. 395–396, 398, and 405 of ref. 21 for details). In the IPESD models, the velocity, pressure, and temperature have the form

$$\begin{aligned} \theta &= \bar{\theta}(\varepsilon x, y, z, t) + \theta'(\varepsilon x, x, y, z, t) + O(\varepsilon) \\ P &= \bar{P}(\varepsilon x, y, z, t) + p'(\varepsilon x, x, y, z, t) + O(\varepsilon) \\ U &= \bar{U}(\varepsilon x, y, z, t) + u'(\varepsilon x, x, y, z, t) + O(\varepsilon) \quad [1] \\ V &= v'(\varepsilon x, x, y, z, t) + \varepsilon \bar{V}(\varepsilon x, y, z, t) \\ W &= w'(\varepsilon x, x, y, z, t) + \varepsilon \bar{W}(\varepsilon x, y, z, t). \end{aligned}$$

The expansion in Eq. 1 is nondimensionalized, with the intraseasonal time scale T_1 as the basic time unit, the equatorial synoptic scale as the basic unit for x, y , and $X = \varepsilon x$, the zonal planetary scale; the height of the troposphere defines the vertical length scale so that vertical motions are much weaker than horizontal motions. In Eq. 1 and below, the zonal average over the equatorial synoptic scale of a general function $g(\varepsilon x, x, y, z, t)$ is defined by

$$\bar{g}(X, y, z, t) = \lim_{L \rightarrow \infty} \frac{1}{2L} \int_{-L}^L g(X, x, y, z, t) dx. \quad [2]$$

In standard notation from turbulence theory, $\bar{g}(X, y, z, t)$ denotes the large-scale mean variables that do not involve fluctuations on the x scale directly, and $g'(X, x, y, z, t)$ denotes a variable with zero large-scale average, i.e., $\bar{g}' = 0$. Thus, the decomposition in Eq. 1 separates the dynamic variable into large-scale envelope means and separate fluctuations on the equatorial synoptic scales. The systematic derivation of the IPESD models from ref. 21 establishes that the fluctuations satisfy the synoptic-scale equatorial weak temperature gradient (SEWTG) equations with zero mean heating on the synoptic scales:

$$\begin{aligned} p'_z &= \theta, & -yv' + p'_x &= 0, \\ w' &= S^\theta, & yu' + p'_y &= 0, \\ \bar{S}^\theta &= 0, & u'_x + v'_y + w'_z &= 0. \end{aligned} \quad [3]$$

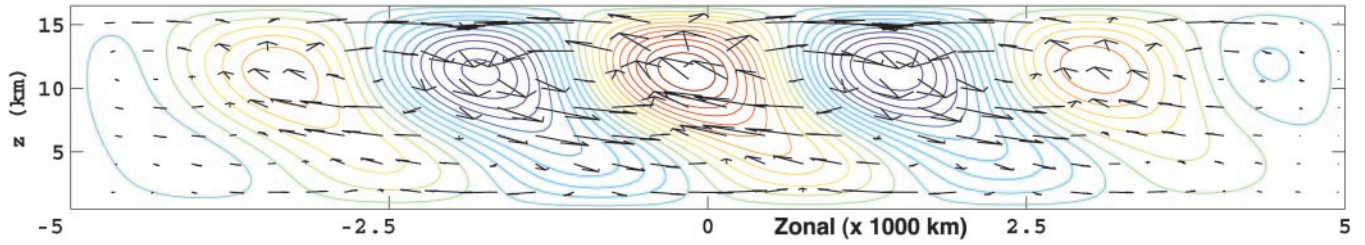


Fig. 1. Contours of synoptic-scale heating (red), cooling (blue), and velocity vectors above the equator as a function of x and z for a westward-tilted ($\phi_0 = \pi/4$) supercluster.

The large-scale envelope variables satisfy the quasilinear equatorial long-wave equations (QLELWE),

$$\begin{aligned} \bar{U}_t - y\bar{V} + \bar{P}_x &= F^U - d\bar{U} \\ \bar{\theta}_t + \bar{W} &= F^\theta - d_\theta\bar{\theta} \\ y\bar{U} + \bar{P}_y &= 0 \\ \bar{P}_z &= \bar{\theta} \\ \bar{U}_x + \bar{V}_y + \bar{W}_z &= 0, \end{aligned} \quad [4]$$

where the forcing terms, F^U and F^θ , are calculated from the turbulent zonal momentum and temperature fluxes,

$$\begin{aligned} F^U &= -\overline{(u'v')_y} - \overline{(u'w')_z} \\ F^\theta &= -\overline{(\theta'v')_y} - \overline{(\theta'w')_z}. \end{aligned} \quad [5]$$

In this article, for simplicity, the coefficients d and d_θ of momentum and thermal damping are set equal below corresponding to a damping time defined by T_1 , i.e., ≈ 3.5 days, which is a standard value used in other studies. The formulas in Eqs. 3–5 define the IPESD models used below.

The IPESD models are systematically derived, simplified multiscale models where, as is evident from Eqs. 1, 4, and 5, the turbulence closure across scales is derived systematically. Furthermore, the IPESD equations are nonlinear but can be solved through two linear equations in a “quasilinear” fashion. As noted in ref. 21, the SEWTG equations in Eq. 3 are solved exactly so that the forcing F^U and F^θ for QLELWE are evaluated explicitly through Eq. 5. The QLELWE in Eq. 4 are then solved by spectral expansion techniques (26). Furthermore, the IPESD models readily allow for zonal flow velocities of order 10 ms^{-1} and heating sources S^θ with the magnitude of 5 K per day (21), reasonable for the equatorial synoptic-scale dynamics and their corresponding convective forcings. These are the values that emerge from the conservative choice of $\varepsilon = 0.125$, which is utilized below to interpret the IPESD solutions. In particular, if the form of the thermal forcing S^θ for SEWTG in Eq. 3 is

$$\begin{aligned} S^\theta &= Q(x, y, z)F(X) \\ Q(x, y, z) &= G_x^1(x, y, t)\sin(z) + G_x^2(x, y, t)\sin(2z) \end{aligned} \quad [6]$$

and involves first and second baroclinic vertical heating modes $\sin(z)$ and $\sin(2z)$, then the exact solution of SEWTG is given by

$$\begin{aligned} u' &= -[(2G^1 + yG_y^1)\cos(z) + 2(2G^2 + yG_y^2)\cos(2z)] \\ v' &= y[G_x^1\cos(z) + G_x^2\cos(2z)] \\ w' &= G_x^1\sin(z) + G_x^2\sin(2z) \\ p' &= y^2[G^1\cos(z) + 2G^2\cos(2z)] \\ \theta' &= -y^2[G^1\sin(z) + 4G^2\sin(2z)]. \end{aligned} \quad [7]$$

Model for Synoptic-Scale Fluctuations in the Warm Pool

The IPESD models enable one to compute the envelope response on planetary scales to balanced equatorial synoptic-scale circulations on intraseasonal time scales. The main premise advanced here is that balanced equatorial synoptic-scale fluctuations that capture key features of the organized behavior of superclusters from F, G, and H yield a planetary response through QLELWE in Eqs. 4 and 5, which captures significant features of the planetary-scale MJO envelope. Here a simple model for the equatorial synoptic-scale fluctuations is developed. First, the observational fact in D suggests that the synoptic-scale fluctuations should be driven by latent heating, and this is why source terms with the form in Eq. 3 with S^θ are assumed in SEWTG to represent the fluctuations. The equatorial Pacific warm pool is centered on the Indonesian marine continent and spans $\approx 10,000 \text{ km}$, from a significant part of the Indian Ocean through the Western Pacific. Equatorial synoptic-scale activity is idealized here as occurring locally in the warm pool by the large-scale modulation function in Eq. 6, $F(X) = \cos(\pi X/2L)^+$, the first positive range of a cosine centered at the origin with L chosen so that the support spans $10,000 \text{ km}$, i.e., $L = 5,000 \text{ km}$. Clearly, the warm pool has continuous fluctuating deep convective activity that supplies latent heating on equatorial synoptic scales. Both observations (27) and theory (24, 25, 28) suggest that first baroclinic heating, the term proportional to $\sin(z)$ in Eq. 6, is ubiquitous in the warm pool and yields a dominant spectral peak. Also, stratiform heating, the term proportional to $\sin(2z)$ in Eq. 6, is significant for organized convective activity both on equatorial mesoscales of order $1,000 \text{ km}$ and equatorial synoptic scales, and yields the other significant spectral peak. In fact, simple models (24, 25, 28) indicate how the structure of equatorial synoptic superclusters can be modeled in a fashion consistent with all the features in F, G, and H from observations through time-lagged stratiform heating. Here we utilize the simplest model for heating fluctuations consistent with all of these features and motivated by the models for superclusters (24, 25, 28). Thus, Q in Eq. 6 is given the form

$$Q = H(y)[\cos(x - \phi(t))\sin(z) - \alpha \cos(x - \phi(t) + \phi_0)\sin(2z)], \quad [8]$$

where $\phi_0 = \pi/4$ is a delayed stratiform phase shift, α , $0 < \alpha < 1$ is the strength of the stratiform heating relative to the direct deep convective heating, and $\phi(t)$ is an arbitrary wave speed. The parameter α is crucial here: for $\alpha = 0$ there is only ubiquitous first baroclinic heating in the warm pool, whereas when $\alpha > 0$ there is significant synoptic-scale stratiform heating in the warm pool due to organized convective activity. Note that the source terms for Eq. 3 with the form Eq. 8 in Eq. 6 automatically satisfy the condition $\bar{S}^\theta = 0$ from Eq. 3. The corresponding balanced SEWTG circulation anomaly with the value $\alpha = 2/3$ for stratiform heating tilted with $\phi_0 = \pi/4$ and with the horizontal structure profile $H(y) = e^{-2y^2}$ centered at the equator is shown in Fig. 1. Fig. 1 depicts the zonal and vertical flow and heating

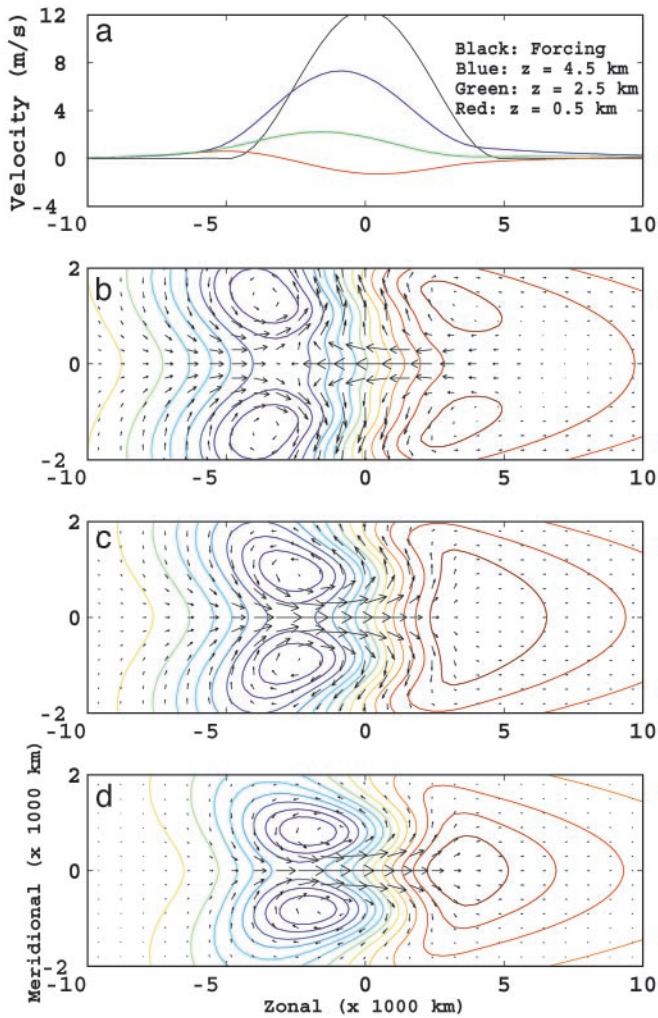


Fig. 4. (a) Forcing amplitude (nondimensional units) and velocity along the equator at different heights for the periodically forced case. Velocity vectors/pressure contours at heights 0.5 km (b), 2.5 km (c), and 4.5 km (d) at 54 days are shown. The vectors and contours are scaled to their maximum magnitude at each height: 1.3 ms^{-1} (b), 2.2 ms^{-1} (c), and 7.4 ms^{-1} (d), respectively.

synoptic-scale organized activity on this intraseasonal time scale. A simple way to do this is to allow $\alpha(t)$ in Eqs. 8 and 9 to begin at zero at time $t = 0$ and vary periodically with period of 40 days through a positive phase of organized convective activity and compute the planetary-scale response through Eqs. 4 and 5. The choice $\alpha(t) = (1 - \cos(\omega_0 t))$ with $\omega_0 = 2\pi/40$ days is utilized below. These results are reported next.

Fig. 3 gives the time history of the zonal flow planetary-scale response in the lower troposphere at the three heights, $z = .5$ km, $z = 2.5$ km, and $z = 4.5$ km. In all figures below, the x, y scales are in units of 1,000 km with the warm pool centered at $x = 0$ and extending over $|x| \leq 5,000$ km; the meridional and zonal velocities are rescaled from their dimensional values according to the domain ratio to aid visualization. At the lowest levels in the free troposphere there are leading low-level easterlies developing, followed by westerlies at the trailing edge of the envelope. At the upper levels of the lower troposphere, much stronger leading westerlies develop and penetrate further eastward during the burst phase of organized convective activity generating strong low-level vertical shear lagging by a few days the maximum of $\alpha(t)$. This behavior is clearly that of a standing wave pattern with a frequency of 40 days and a structure as in

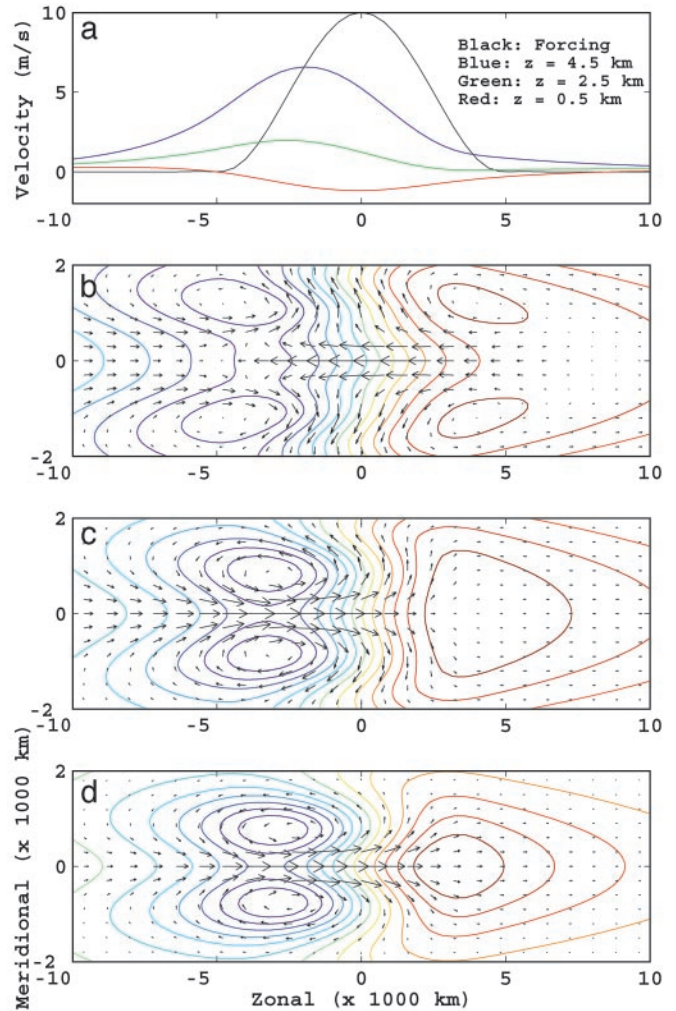


Fig. 5. Same as Fig. 4 except for a forcing envelope traveling eastward at 5 ms^{-1} . Maximum velocity magnitudes: 1.5 ms^{-1} (b), 2 ms^{-1} (c), and 6.5 ms^{-1} (d).

E. Fig. 4 depicts the flow field and pressure at 54 days that is representative of the build-up phase of the organized synoptic-scale activity as $\alpha(t)$ goes from zero at 40 days to its maximum at 60 days. Fig. 4 shows clear evidence of a strong “westerly wind event” developing on planetary scales with features resembling the observational characteristics of the MJO in A and E. The lowest vertical level of the troposphere here at 0.5 km displays the characteristic planetary-scale structure of the low levels of the MJO in observations from A and E with a clear pair of leading cyclones and trailing anticyclones, whereas at the levels $z = 2.5$ and 4.5 km the westerly wind burst strengthens with height and invades the envelope region, generating strong low-level vertical shear. This standing wave envelope clearly captures several of the observed features in A and E in a transparent qualitative fashion and develops as a quantitative result of C in the multiscale models. Figs. 3 and 4a show that this standing wave is formed in the western part of the warm-pool envelope, i.e., in the Indian Ocean, as in B. Also, as is evident from Fig. 4, the standing wave phase has a strong equatorial Rossby wave (26) component with a 40-day period. This simple example suggests the possible fashion in which the low-frequency equatorial Rossby wave part of the spectrum from I can be generated through such standing wave activity on planetary scales through organized synoptic-scale circulations but without sufficient intensity to generate a propagating MJO.

A Propagating MJO Envelope

One feature of the MJO not captured by the solutions just presented is their propagation phase speed. The simplest way to introduce a propagation speed into the multiscale models is to assume that the warm-pool envelope, F , moves at a speed s , i.e., use $F(X - st)$ in Eqs. 6, 8, and 9 rather than a fixed $F(X)$. In this context, it is also natural to assume that α is a specified constant so that the propagating large-scale wave that emerges from the multiscale model is created by a fixed level of balanced equatorial synoptic-scale wave activity consistent with a supercluster wave train. Here, α is fixed at the value $2/3$ and all other parameters of the SEWTG heating are the same as presented earlier. The propagation speed for the warm-pool envelope is specified as an eastward velocity of 5 ms^{-1} as for the MJO. The resulting planetary response moving at 5 ms^{-1} is given in Fig. 5. The flow field displays nearly the identical structure to the standing wave pattern that formed *in situ* in Fig. 4. Thus, this planetary-scale response has several features of the MJO large-scale envelope from A, B, and E and has been created from a simplified multiscale model for the upscale transport of kinetic and thermal energy of organized equatorial synoptic-scale wave trains having key features of the observational record regarding superclusters.

Concluding Discussion

In the present article a multiscale model has been developed as a simplified model that clearly demonstrates the fashion in which planetary-scale circulations sharing many features with the MJO envelope are generated on intraseasonal time scales through wave trains of organized synoptic-scale circulations having many features in common with superclusters. The appeal of the present theory is its firm mathematical underpinnings, simplicity, and analytic tractability while remaining self-consistent with many features of the observational record for tropical intraseasonal variability. Although the theory is nonlinear, it is actually “quasilinear” and is analyzed by exactly solving linear problems in two stages. In the first stage, a process model for equatorial synoptic-scale circulations in the warm pool is developed; this is an obvious place for further development and exploration of the models. In the second stage, the multiscale model provides a rigorous asymptotic closure for zonal momentum and thermal fluxes that are calculated explicitly from the synoptic-scale fluctuations. In this stage, the planetary response is computed by

solving the linear equatorial long-wave equations with known momentum and thermal forcings. In this last stage, the equations resemble superficially those of Chao (15) in the linear moving heat source model of the MJO that is based on the Gill model (29) for circulations induced by heating; however, the interpretation and derivation is completely different here, with both planetary-scale momentum forcing, F^U , and thermal forcing, F^θ , generated through derived synoptic-scale fluxes with momentum forcing dominating the response rather than just specifying some arbitrary moving heating as in ref. 15. The genuine multiscale models for the MJO developed here share a common theme with Moncrieff's (16) interesting recent phenomenological theory for the upscale transport of momentum from equatorial mesoscales, $O(300 \text{ km})$, to planetary scales. In detail, the two approaches are quite different, with the present models focusing on the transfer of kinetic and thermal energy from equatorial synoptic scales to planetary scales with a systematic derived closure principle for the large-scale envelope with planetary responses allowing for equatorial Kelvin waves (26) as in the low-level easterly flow in Figs. 4 and 5 and Rossby waves. Moncrieff's models rely on a phenomenological closure principle for momentum alone and do not allow for any equatorial synoptic-scale behavior or Kelvin-wave behavior in the planetary-scale response but yield an interesting nonlinear eigenvalue problem for the wave speed of traveling waves. Nevertheless, the common theme of the two approaches is that the upscale transport of momentum and temperature is crucial in the accurate representation of the MJO. The present theory suggests that accurate representation of coherent superclusters is a crucial feature needed for contemporary GCMs to resolve the MJO. The work here suggests that more systematic studies like that of Moncrieff and Klinker (30) are needed to understand this issue in GCMs.

Many aspects of the basic multiscale models presented here merit further investigation, including the role of dissipation parameters, boundary layer friction, and changes in the warm-pool synoptic-scale model. It is also interesting to develop “mild closure” models where the large scales can influence the shape of the warm-pool envelope.

The research of A.J.M. is partially supported by Office of Naval Research Grant ONR N00014-96-1-0043 and National Science Foundation Grants NSF DMS-96225795 and NSF-FRG DMS-0139918. J.A.B. is supported as a postdoctoral research associate with A.J.M. through National Science Foundation Grant NSF-FRG DMS-0139918.

- Madden, R. & Julian, P. (1972) *J. Atmos. Sci.* **29**, 1109–1123.
- Nakazawa, T. (1988) *J. Meteor. Soc. Japan* **66**, 823–839.
- Hendon, H. & Salby, M. (1994) *J. Atmos. Sci.* **51**, 2225–2237.
- Hendon, H. & Leibmann, B. (1994) *J. Geophys. Res.* **99**, 8073–8083.
- Maloney, E. & Hartmann, D. (1998) *J. Climate* **11**, 2387–2403.
- Madden, R. A. & Julian, P. (1994) *Mon. Weather Rev.* **122**, 814–837.
- Vecchi, G. & Harrison, D. E. (2000) *J. Climate* **11**, 1814–1830.
- Zhang, C. & Anderson, S. (2003) *J. Atmos. Sci.* **60**, 2196–2207.
- Sperber, K. R., Slingo, J. M., Inness, P. K. & Lau, K.-M. (1997) *Clim. Dynam.* **13**, 769–795.
- Emmanuel, K. A. (1987) *J. Atmos. Sci.* **44**, 2324–2340.
- Neelin, J. D., Held, I. M. & Cook, K. H. (1987) *J. Atmos. Sci.* **44**, 2341–2348.
- Wang, B. & Rui, H. (1990) *J. Atmos. Sci.* **47**, 397–413.
- Salby, M., Garcia, R. & Hendon, H. (1994) *J. Atmos. Sci.* **51**, 2344–2367.
- Raymond, D. J. (2001) *J. Atmos. Sci.* **58**, 2807–2819.
- Chao, W. C. (1987) *J. Atmos. Sci.* **44**, 1940–1949.
- Moncrieff, M. (2004) *J. Atmos. Sci.*, in press.
- Grabowski, W. W. (2001) *J. Atmos. Sci.* **58**, 978–997.
- Wheeler, M. & Kiladis, G. N. (1999) *J. Atmos. Sci.* **56**, 374–399.
- Wheeler, M., Kiladis, G. N. & Webster, P. (2000) *J. Atmos. Sci.* **57**, 613–639.
- Straub, K. H. & Kiladis, G. N. (2002) *J. Atmos. Sci.* **59**, 30–53.
- Majda, A. J. & Klein, R. (2003) *J. Atmos. Sci.* **60**, 393–408.
- Yanai, M., Chen, B. & Tung, W.-W. (2000) *J. Atmos. Sci.* **57**, 2374–2396.
- Lin, X. & Johnson, R. (1996) *J. Atmos. Sci.* **53**, 695–715.
- Majda, A. J. & Shefter, M. G. (2001) *J. Atmos. Sci.* **58**, 1567–1584.
- Majda, A. J., Khouider, B., Kiladis, G., Straub, K. & Shefter, M. (2004) *J. Atmos. Sci.*, in press.
- Majda, A. J. (2003) *Introduction to PDEs and Waves for the Atmosphere and Ocean*, Courant Institute Lecture Series 9 (Amer. Math. Soc., Providence, RI), Chap. 9.
- Mapes, B. E. & Houze, R. A. (1995) *J. Atmos. Sci.* **52**, 1807–1828.
- Mapes, B. E. (2000) *J. Atmos. Sci.* **57**, 1515–1535.
- Gill, A. E. (1980) *Quart. J. R. Meteor. Soc.* **106**, 447–462.
- Moncrieff, M. & Klinker, E. (1997) *Q. J. R. Met. Soc.* **123**, 805–827.